Selective Area Laser Deposition - A Method of Solid Freeform Fabrication

W. Richards Thissell, Guisheng Zong, James Tompkins,
Britton R. Birmingham, and Harris L. Marcus

Center for Materials Science and Engineering
ETC 9.104
The University of Texas at Austin
Austin TX 78712
(512) 471-1504
FAX: (512) 471-7681

Selective area laser deposition (SALD) is a mechanism by which solid material may be deposited from the gas phase in a controlled area. This paper describes the mechanism of SALD and discusses the advantages and disadvantages of using SALD for achieving SFF. Several interesting problems currently inhibiting the use of SALD for SFF are described and potential solutions to these problems are proposed. Included is a discussion of the continuing development of the SALD processing machine capability.

I.Table of Symbols

$\mathbf{c}_i$	Random velocity vector of species i
c_i	Magnitude of random velocity of species i, $\frac{m}{s}$ $c_i = \mathbf{c}_i \cdot \mathbf{c}_i$
E_{a_i}	Activation energy of reaction i, $\frac{J}{mole}$
F	Random velocity distribution, $\frac{species\ s}{m^4}$
f	Kinetic energy distribution function, dimensionless
f^*	Isotropic kinetic energy distribution function, dimensionless
k_{f_i}	Forward rate constant of reaction i, depends on reaction i
k_{o_i}	Pre-exponential factor for reaction rate constant i, depends on reaction i
M_i	Molar mass of species i, $\frac{kg}{mole}$
N_o	Avogadro's Number, 6.022×10^{23} $\frac{species}{mole}$
n_i	Number density of species i, $\frac{species}{m^3}$
P_{Laser}	Effective laser power at substrate, W
$\mathbf{r}$	Spatial position vector
r_n	Radius of nuclei, m
R	Gas Constant, $8.314 \frac{J}{mole\ ^oK}$
R_n	Rate of nucleation, $\frac{1}{m^3}$
s	Step size between adjacent laser scan lines, m
T	Temperature, °K

T_o	Reference temperature, 298 °K
t	Time, second
$\boldsymbol{u}_i$	Average macroscopic fluid velocity vector for species i, $\boldsymbol{u}_i = \langle v \rangle_i$
$\boldsymbol{v}$	Fluid velocity space vector, $\boldsymbol{v} = \boldsymbol{c}_i + \boldsymbol{u}_i$
v_s	Magnitude of the velocity between the laser beam and substrate, $\frac{\mathrm{m}}{\mathrm{s}}$
Z_i	Collision frequency of species i, $\frac{\mathrm{species}}{\mathrm{m}^2}$
β_i	Temperature exponent in reaction rate constant i, dimensionless
γ_{dv}	Surface Gibb's free energy between deposit and vapor, $\frac{\mathrm{J}}{\mathrm{m}^2}$
κ	Boltzmann constant, $\kappa = 1.380 \times 10^{-23} \frac{\mathrm{J}}{\mathrm{species}\cdot\mathrm{K}}$
η'	Sticking coefficient, dimensionless
ρ	Density, $\frac{\mathrm{kg}}{\mathrm{m}^3}$

II.Gas Phase Solid Freeform Fabrication

Selective area laser deposition (SALD) is a method of achieving SFF from the gas phase.[1,2] This method results in parts that are totally deposited from the gas phase. SALD, like all gas phase deposition processes, has the potential to be employed to deposit a wide range of thermodynamically stable and metastable materials, including highly cross-linked polymers, metals, ceramics, carbon based materials ranging from amorphous sp^2 and sp^3 bonded carbon to graphite and diamond, and composites of these materials. The deposits may be either amorphous or crystalline. The deposits can be fully dense when the deposition mechanism occurs on a surface, but they can contain residual porosity when the deposition mechanism is homogenous gas phase nucleation via gas phase formation of polycylic aromatic compounds, followed by nucleus adsorption and densification through mesophase.[3] SALD is highly suitable for computer automation and control, thereby permitting its use as a method for achieving SFF. Arbitrary overhangs may be achieved by first depositing a sacrificial material from the gas phase, followed by deposition of the desired material. The sacrificial material may then be removed by appropriate chemical or physical treatment. Arbitrary shapes may also be made by SALD by either scanning two orthogonal beams over a substrate stage that can rotate around the incident axis of one beam, or by a fixed beam and an n degree of freedom robotic stage where n may be as high as six.

A.SALD Mechanism

The SALD mechanism is a laser induced chemical vapor deposition process on or over a substrate. The deposition mechanism may be either pyrolytic or photolytic. Pyrolytic deposition may be achieved by focusing a laser beam to a small waist at a substrate surface. The laser beam is moved relative to the surface. The surface material and laser wavelength are chosen so that the photon energy is absorbed by the substrate, resulting in phonon heating of the substrate. The beam intensity and beam scan velocity are chosen so that the substrate heating remains localized and the temperature of the substrate results in deposition at the surface. The beam waist is chosen to achieve the desired beam intensity for a given laser

output power and a given part feature resolution. The deposit diameter is usually less than the beam diameter due to Arrhenius reaction kinetics. For high substrate heating situations, the substrate at the center of the beam waist may be hot enough to result in substrate or deposit melting or vaporization and the deposit width may be greater than the beam waist due to heat conduction to the surrounding area.

Photolytic deposition may also be used in SALD to achieve SFF. One potential embodiment of photolytic deposition is the photolytic activation of certain gas phase chemical species, followed by subsequent selective deposition on a laser heated substrate. SALD research has not yet begun on this approach.

The key identified issues in SALD include proper nucleation and a high nucleation density, fast and microstructurally controllable chemical deposition kinetics, real time growth rate control and measurement, arbitrary substrate or beam positioning, computer controlled laser power, and real time laser heated spot temperature measurement. Two of these issues, nucleation phenomena and fast chemical kinetics will be discussed in more detail in this paper.

1.Nucleation Phenomena in SALD

Nucleation refers to the establishment of material nuclei of a critical size.[4] Nuclei smaller than the critical size are energetically unstable due to having a high surface free energy relative to the internal free energy of the material. The nuclei smaller than the critical size have a much higher probability to disappear than to grow further. Nuclei that are at the critical size have a differential change in surface free energy equal to a differential change in internal free energy of the material, and therefore it is as probable that they will disappear as it is probable that they will grow further. Nuclei larger than the critical nucleus size will grow spontaneously.

Deposition from the gas phase is preceded by the establishment of critically sized nuclei of the deposition material. Creating conditions that favor either the establishment of critically sized nuclei include supersaturating the vapor phase with chemical species that either react to form the deposit material on a surface or are indeed embryonic nuclei of the deposition phase. Catalytic efforts that act to decrease the size of critically sized nuclei also increase the nucleation density.

The largest critically sized nuclei occur in homogenous gas phase nucleation, where the nuclei form approximate spheroids, having a rate of formation that may be approximated by:

$$R_n \cong Z\,\eta'(4\pi r_n^2)\,e^{\frac{-2\gamma_{dv}}{r_n}\frac{4\pi r_n^3}{3\kappa T}} \tag{1}$$

where Z, the collision frequency in a single component vapor phase of supersaturated vapor molecules with the nucleus surface, is given by:

$$Z_i = \frac{1}{4} n_i \sqrt{\frac{8\kappa N_o T}{\pi M_i}} \tag{2}$$

assuming that the vapor is at thermodynamic equilibrium. From inspection of equation 1, the rate of formation of nuclei of radius r_n from supersaturated vapor first increases with increasing r_n due to increasing collision and sticking of vapor molecules to the nuclei. The rate of formation then decreases with further increases in r_n due to the exponential term which represents the energy associated with forming large nuclei. However, once stable nuclei are formed, their continued growth occurs by chemical or phase deposition kinetics, which is not described by equation 1. Inspection of equation 2 shows that the rate of nuclei formation increases linearly with increasing pressure. Figure 1 shows amorphous carbon that was deposited using SALD from 99.6% acetylene plus acetone (solvent). Note the truncated spherical shape of the deposit particles that may be indicative of gas phase nucleation at the laser heated substrate. The smoothing out of the round particles upon contact with other particles can be explained if the particles were still in the mesophase state upon adsorption with the deposit surface. The residual porosity between groups of particles may indicate that much of the growth occurs in the gas phase before nucleus adsorption onto the deposit surface. The presence of the small lighter colored particles on the larger darker colored particles are probably newer nuclei that have densified less than the larger nuclei. The separation of whether nucleation occurs on or near the deposition surface still requires clarification.

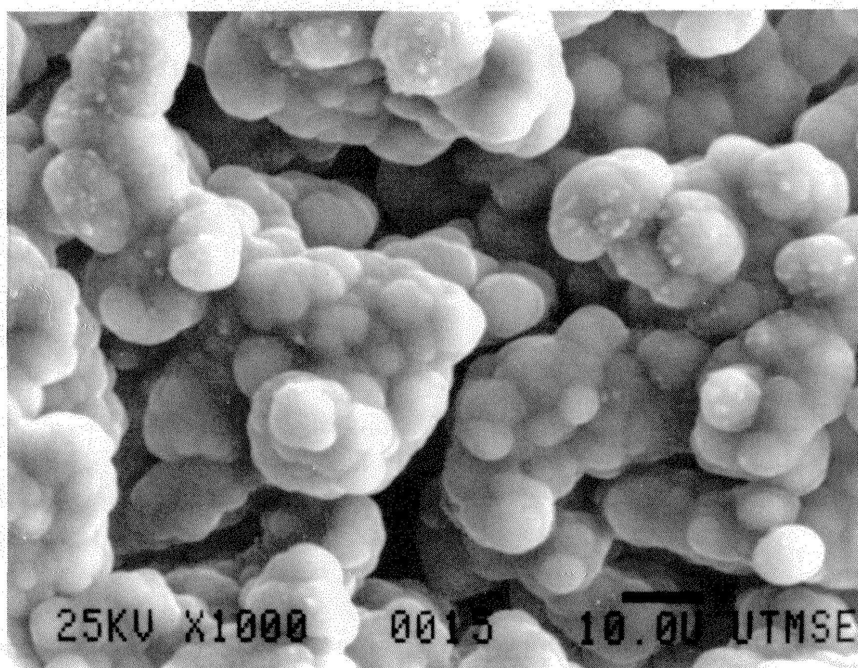

—— 10 μm

Figure 1: SALD of carbon from 500 Torr C_2H_2. P_{Laser} = 3 W. $v_s = 1x10^{-3}\ \frac{m}{s}$, 12,500 laser scans on SiC powder substrate.

Deposit nucleation on surfaces is similar to vapor condensation on surfaces with respect to a decrease in supersaturation required to reach the critical nucleus size when compared to homogeneous gas phase nucleation. In both cases the surface acts to decrease the size of the critically sized nucleus relative to the homogeneous gas phase case, for a

given set of vapor phase conditions, if the surface has a surface free energy similar to that of the deposit or liquid. The amount of the decrease in critical nucleus size relative to the homogeneous gas phase nucleation case is a function of the difference in surface free energy between the deposit and the surface upon which it is nucleating, and the geometry of the nucleating surface site. Surface nucleation and growth is preferable to homogeneous gas phase nucleation for SALD of cohesive, tough parts because it can lead to denser deposits. Figure 2 shows surface nucleation that results in dense deposition. The hemispherical high spots on the surface result from instabilities in the deposition process. A differential increase in surface height leads to a differential decrease in heat transfer to the bulk. This results in a differential increase in surface temperature at the high spot. This leads to a differential increase in deposition rate which is further enhanced in this case by an increase in reactant concentration away from the surface.

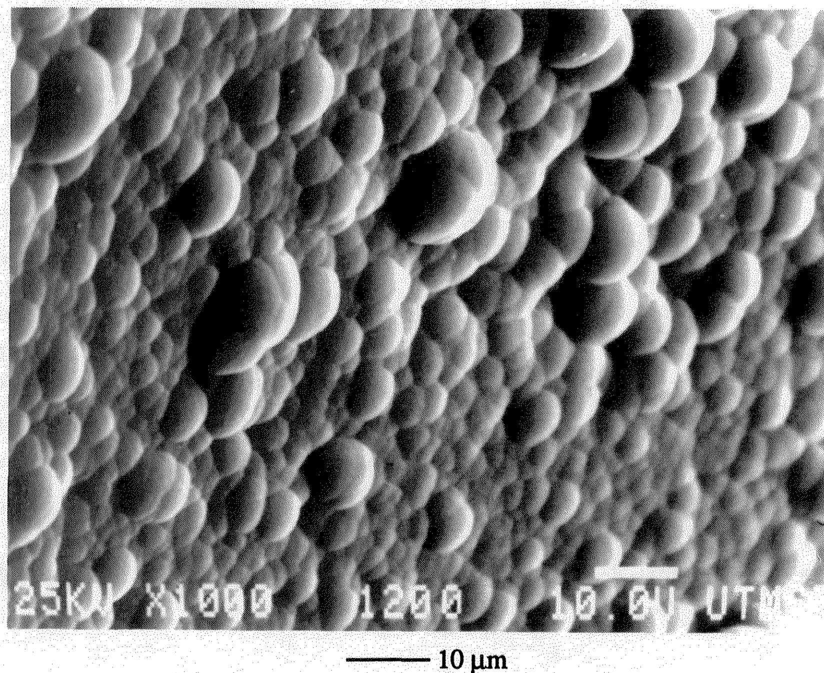

—— 10 µm

Figure 2: SALD carbon from 700 Torr C_2H_2. The substrate is SiC powder. P_{Laser} = 5 W. $v_s = 1\mathrm{x}10^{-3}\ \frac{\mathrm{m}}{\mathrm{s}}$, $s = 5\mathrm{x}10^{-5}$ m.

A high nucleation density is required for SFF from SALD in order to achieve layered deposits. A low nucleation density results in localized deposition whereas a high nucleation density results in the nuclei growing together and forming a dense layer. Figure 3 shows a very low nucleation density of carbon on bulk Al_2O_3. The lighter colored deposits are small are sparse on the substrate, with essentially no contact with each other.

2.Chemical Kinetics and SALD

Gas phase SFF using SALD requires fast deposition kinetics in order to achieve macroscopically meaningful deposits in economical time periods. The faster the deposition rate for desirable microstructures the better.

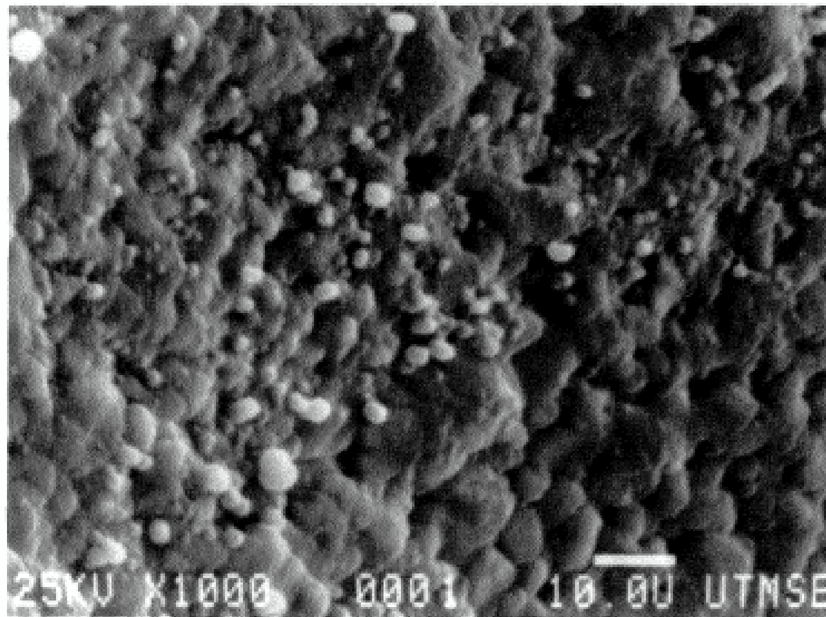

——— 10 µm

Figure 3: SALD carbon from 200 Torr C_2H_2. The substrate is bulk Al_2O_3. The lighter colored round shapes are the deposit. $P_{Laser} = 6$ W. $v_s = 5.08 \times 10^{-4} \frac{m}{s}$, $s = 12.7 \times 10^{-5}$ m.

Certain materials, such as arbitrary sp^3 bonded carbon parts, cannot currently be made by any method because it is impossible to machine, cast, extrude, mold, *etc.* with this material. Therefore, SFF using SALD of sp^3 bonded carbon is especially attractive because of the supreme material property uniqueness of sp^3 bonded carbon and the lack of alternative manufacturing methods for it. An additional advantage with carbon deposition as the initial SALD process system is that most of the process gases for carbon deposition are much safer to handle, with the exception of optional halogens, than process gases for certain other material deposition processes such as SiC or Si_3N_4.

Linear carbon rod growth rates of up to 1 mm/s have been observed.[5] The microstructure and carbon bonding type of deposits deposited at this rate have not been studied in detail. Large area good quality diamond film deposition has been achieved at rates of up to 930 µm/hr,[6] and deposition rates have increased several orders of magnitude in the past decade. Further increases in sp^3 bonded carbon deposition rates are likely, but the next decade is not likely to lead to another increase of several orders of magnitude.

Engineering and controlling high deposition rates requires knowledge of the reaction pathway from initial feed gases to final deposition products. This knowledge permits the implementation of design strategies that increase the concentration of desirable species and decrease the concentration of undesirable species. The desirability of a given species is related to whether it enhances (desirable) or inhibits (undesirable) the rate of deposition either directly or indirectly.

Traditional CVD techniques rely on thermodynamic equilibrium to produce chemical species with sufficient energy to overcome the activation energy barrier for a given reaction. The energy available to overcome the activation energy barrier is the sum of the kinetic and internal energy of the reactants. Most of the atomic and molecular kinetic energy results from the random velocity component, while the potential energy is the sum of vibrational energy, rotational energy, excited metastable energy, and unpaired electrons (free radicals). Kinetic energy may be transferred to internal energy via inelastic collisions, while potential energy may be transferred to kinetic energy via superelastic collisions. The distribution of random velocity for processes at or very near equilibrium and not under applied external forces is given by a local Maxwell-Boltzmann distribution function integrated over a differential volume sphere in velocity space:[7]

$$\mathcal{F}(\boldsymbol{r}, c, t) = 4\,\pi c^2 n_i(\boldsymbol{r}, t)\left(\frac{M_i}{2\pi N_o \kappa T_i(\boldsymbol{r}, t)}\right)^{\frac{3}{2}} e^{\frac{-M_i(v - u_i(r,t))^2}{2 N_o \kappa T_i(r,t)}} \tag{5}$$

The concept of temperature is defined only for populations that have random velocity distributions that can be described by the Maxwell-Boltzmann distribution function. The temperature of a chemical species is thus defined as:

$$T_i = \frac{M_i}{3 N_o \kappa} < c_i^2 > \tag{6}$$

where $< c_i^2 >$ is the average of the square of the magnitude of the random velocity and is given by:

$$< c_i^2 > = \frac{1}{n_i}\int_{-\infty}^{\infty} c_i^2\, f \mathrm{d}\boldsymbol{v} \tag{7}$$

Chemical reactions can be assumed to have rate constant dependencies that can be expressed as:

$$k_{f_i} = k_{o_i}\left[\frac{T}{T_o}\right]^{\beta_i} e^{\frac{-E_{a_i}}{RT}} \tag{8}$$

As an example, let us look at the kinetics of pyrolytic carbon deposition from acetylene. A first order rate constant for this reaction has the following rate constants in the temperature range of 820-1375 °K:[8]

$$k_{o_i} = 17.1 \times 10^{-6} \left[\frac{\mathrm{kg}}{\mathrm{m^2\,s\,Pa}}\right]$$

$$\beta = 0$$

$$E_a = 138 \quad \left[\frac{\mathrm{kJ}}{\mathrm{mole}}\right]$$

Pyrolytic carbon deposition from acetylene is not a one step reaction, but includes many individual reactions. Overall reaction rate equations are process and temperature range specific. The constants given above result most likely from the rate limiting step in the particular reaction pathway. Figure 4 shows a plot of this rate constant with respect to temperature. Conversion to a linear growth rate can be achieved by dividing the ordinate by a nominal density, $\rho = 1.8 \times 10^3 \frac{\mathrm{kg}}{\mathrm{m^3}}$. Note that the rate rises exponentially with temperature. However, very high temperatures are required for an appreciable deposition rate at an acetylene partial pressure of 10^5 Pa. This is because of the high activation energy of the reaction. Figure 5 shows a plot of the Maxwell-Boltzmann velocity distribution of acetylene versus random velocity and temperature. Note that as the temperature rises, the normalized

Maxwell-Boltzmann velocity distribution becomes more broad and the peak shifts to higher molecular velocity levels. However, the fraction of the total population of molecular particles that have enough random velocity to participate in inelastic collisions that can overcome the activation energy of the pyrolytic carbon deposition reaction from acetylene is very small in the temperature range reported in Figure 4.

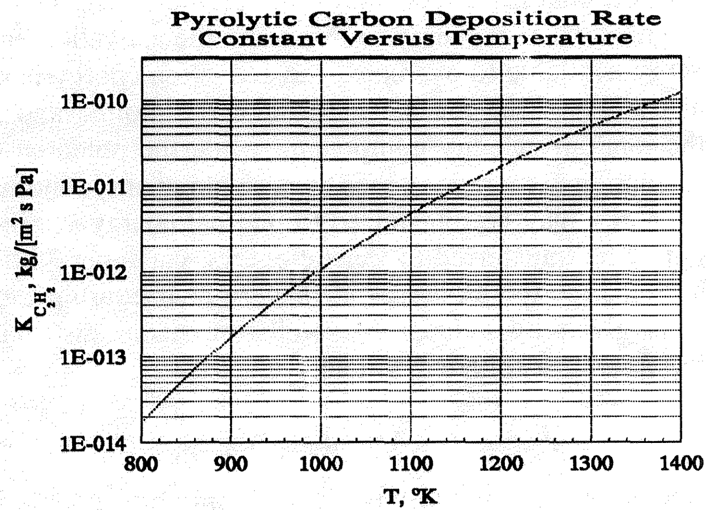

Figure 4: Pyrolytic carbon deposition rate constant versus temperature.

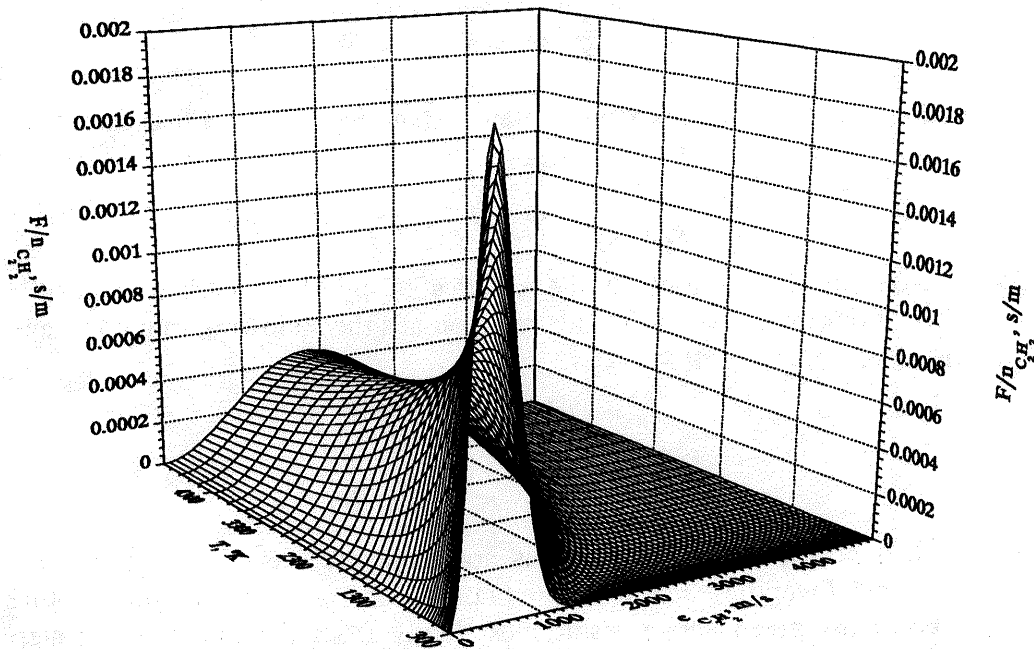

Figure 5: Normalized acetylene random velocity distribution versus random velocity and gas temperature. Random velocity is proportional to the square root of the molecular kinetic energy. The integral of the normalized random velocity distribution function over all velocities is equal to one.

To summarize, for thermal CVD processes, such as pyrolytic carbon deposition from acetylene, the deposition rate in the kinetic rate limited deposition regime increases exponentially with temperature and linearly with the partial pressure of acetylene.

Plasma deposition is more complicated than thermal CVD, but it can provide great increases in deposition rate when compared to thermal CVD at a given substrate temperature, feed gas partial pressures and flow rates. Electron, atomic and molecular species can exist with two very different kinetic energy distribution profiles below about 26-40 kPa of pressure, due to the great difference between the electrons and the others in mass, collision cross sectional area, and ability to accelerate through an electric field. Electrons cannot accelerate to high enough velocities between inelastic collisions at pressures higher than about 300 Torr to maintain a kinetic energy distribution profile significantly higher than the neutral and ionic species. The free electrons are very small relative to atomic and molecular species and they have a very high charge to mass ratio. This allows them to absorb energy from an applied electric field much more efficiently than molecular and atomic ions, which exist in at least the same concentrations as the electrons in volumes greater than the Debye sphere due to the powerful law of electroneutrality. However, the concentrations of ions is very low, about 10^{-5} times the neutral species concentrations in plasmas of interest for deposition, particularly SALD. This category of plasma is called weakly ionized. A further characteristic of these plasmas is that the average kinetic energy of the free electrons is typically below about $9.64 \times 10^5 \frac{kJ}{mole}$ (10 eV=1.16×10^5 °K for a Maxwell-Boltzmann distribution), while the ions and neutrals are typically in thermal equilibrium in the temperature range of 400-600 °K. The average electron kinetic energy is below the ionization threshold of most diatomics and nobles. The electrons with higher energy than particular bond strengths in neutrals and ions may cause bond breakage upon an inelastic collision with a neutral or ion, or excitation to long lived metastable states. Therefore, a weakly ionized plasma can be used to transfer internal energy from energetic free electrons to an ionic and neutral specie population having a relatively low random velocity distribution ("cold"). This can create much higher concentrations of species having sufficient internal energies to overcome the activation energy barriers of many reactions than exist in the case of thermal equilibrium alone. In fact, it is possible to create weakly ionized plasmas where most of the chemical species are radicals and atomic species if recombination reactions are properly controlled. Table 1 lists bond strengths, ionization energies, and metastable energetic states of several gases. Note that N_2 and the noble gases can have excited states above the bond strength of H_2 and O_2. This allows for the creation of internal energy transport regimes in reactors where excited states can transfer internal energy absorbed through inelastic impact with free electrons to a zone where the deposition process gases are introduced. Isolation of the plasma process from the SALD process can be thus achieved.[9]

Sp^3 bonded carbon deposition requires conditions that create high partial pressures of atomic hydrogen and/or oxygen. Such conditions also lead to the formation of many other atomic and molecular species from the feed gases; the analysis and modeling of which is a non-trivial task. The primary source reaction of atomic hydrogen and oxygen is the inelastic collision of an energetic free electron with molecular hydrogen and oxygen. The primary sink reaction of atomic hydrogen and oxygen is the three body recombination reaction of two atomic hydrogen or oxygen atoms. The third body is necessary to absorb the internal energy of the unpaired electrons in the reactants to stabilize the recombination. The third body may be a wall or another gas phase species such as H_20 or CO_2. Wall recombinations have been shown to be a major drain of atomic species created in plasma processes.[10,11] Wall

recombination reaction rates may be decreased by several order of magnitude by appropriate wall plasma treatments and sufficient wall cooling.

Table 1:
Bond Strength, Ionization Energy, And Metastable Energies of Selected Gases

Gas	Bond Strength, $\frac{kJ}{mole}$	Ionization Energy, $\frac{kJ}{mole}$	Reactive State	Metastable Energy, $\frac{kJ}{mole}$	Reference
H_2	433.7	1484.1	$^3\Sigma\mu$,repulsive	878.3	12
O_2	498.6	1802.1	$a^1\Delta_u$	~500	13
			$A^3\Sigma_u^+$	~443	13
			$B^3\Sigma_u^-$	~587	13
N_2			Vibrational	~480-770	12
He			lowest triplet	1908.1	12
Ne			lowest triplet	1601.6	12
Ar			lowest triplet	1113.1	12
CH_3-H	426.9				12
CH_3-CH_3	384.5				12
CH_3-ND_2	244.8				12
CH_3-OH	380.5				12
CH_3-Cl	327.6				12
CH_3-Br	224.5				12
CH_3-I	221.6				12

III.Current Status of SALD Development

Three generations of SALD reactors have been designed and fabricated within the past two years. This third system is designed to both further develop the SALD process towards the goal of achieving solid freeform fabrication, and contribute to the basic science of the nature of carbon deposition from the gas phase that is important to understanding the SALD process, as well as other gas phase deposition processes. Highlights of the SALD system III design have been previously published.[14]

The SALD system III is designed to study the gas phase deposition of *sp*^{3} bonded carbon for both SALD and large area plasma deposition processes. The primary goal of its design is to determine the mechanism of *sp*^{3} bonded carbon deposition through plasma diagnostics and resonance enhanced multiphoton ionization time of flight mass spectroscopy (REMPITOFMS). REMPITOFMS provides a qualitative analysis of the transient gas phase

species directly above a depositing surface. This knowledge will be used to develop methods to increase the deposition rate of sp^3 bonded carbon.

The second generation has been used to obtain high rates of linear carbon deposition from the gas phase. This achievement proves that macroscopically significant amounts of material may be deposited from the gas phase. This system has also made the first SALD parts out of carbon, including rings and blocks with 10^{-3} m dimensions. Experiments with this system have shown several critical areas for research, including deposition rate control and nucleation density.

IV.Conclusion

SALD has the potential to be used to deposit a variety of materials from the gas phase. SALD can be computer controlled so that SFF may be achieved with it. Achieving SFF via SALD requires high rate deposition that can also be well controlled spatially and temporally so that part dimensional tolerance and material properties can be controlled to desired specifications.

High rate controlled deposition requires a fundamental understanding of the complete chemical mechanism from feed gases to deposited material. The addition of plasma chemistry with SALD adds considerable complexity to the vapor phase chemistry, but it can greatly increase the deposition rate when compared to thermal equilibrium processes at the same feed gas partial pressures, flow rates, and substrate temperatures. This is due to electric and magnetic field power coupling to free electrons which transfer the absorbed energy through inelastic collisions with ions and neutrals. It is possible to adjust the nature of this power coupling to produce high concentrations of desirable reactive species by manipulation of the process parameters. Studies will be performed in the next year to explore these possibilities with the SALD system III reactor and plasma diagnostic system.

V.Acknowledgements

This project is sponsored by the Texas Advanced Technology Program.

---

[1] Zong, Guisheng, Robert Carnes, Harovel G. Wheat, and Harris L. Marcus, "Solid Freefrom Fabrication by Selective Area Laser Deposition," Proceedings of The Solid Freeform Fabrication Symposium, edited by J. J. Beaman, H. L. Marcus, D. L. Bourell, and J. W. Barlow, The University of Texas at Austin, Austin Texas, August 6-8, 1990, 83-90.

[2] Zong, Guisheng, Yves Jacquot, W. Richards Thissell, and H. L. Marcus, "Solid Freeform Fabrication Using Selective Area Laser Deposition," Plasma and Laser Processing of Materials, edited by Upadhya, Kamleshwar, TMS, 1991, 23-48.

[3] Marsh, Harry and Philip L. Walker, Jr., "The Formation of Graphitizable Carbons Via Mesophase: Chemical and Kinetic Considerations," in Chemistry and Physics of Carbon, edited by Walker, Peter L., Jr. and Peter A. Thrower, 15, 1979, 229-86.

[4]Hiemenz, Paul C., Principles of Colloid And Surface Chemistry, 2nd edition, New York: Marcel Dekker, Inc., 1986.

[5]See reference 2.

[6] Ohtake, Naoto, Hitoshi Tokura, Yasuhiko Kuriyama, "Synthesis of Diamond Film By Arc Discharge Plasma CVD," Proceedings of the First International Symposium on Diamond and Diamond-like Films, edited by Dismukes, J. P., A. J. Purdes, B. S. Meyerson, T. D. Moustakas, D. E. Spear, F. V. Ravi, and M. Yoder, The Electrochemical Society, 89-12, 1989, 93-105.

[7]Bittencourt, J. A., Fundamentals of Plasma Physics, New York: Pergamon Press, 1988.

[8]Tesner, P. A., "Kinetics of Pyrolytic Carbon Formation," Chemistry and Physics of Carbon, edited by Thrower, Peter A., 19, 1984, 65-161.

[9]W. Richards Thissell, James Tompkins, and Harris L. Marcus, "Design of a Solid Freeform Fabrication Diamond Reactor," Proceedings of The Solid Freeform Fabrication Symposium, edited by J. J. Beaman, H. L. Marcus, D. L. Bourell, and J. W. Barlow, The University of Texas at Austin, Austin Texas, August 6-8, 1990, 48-73.

[10]Fite, W. L., In Chemical Reactions in Electrical Discharges, edited by Blaustein, B. D., *Advances in Chemistry Series*, No. 80, Washington D. C.: American Chemical Society, 1969.

[11]Greaves, J. C. and J. W. Linnett, "Recombination of Atoms at Surfaces: Part 6.-Recombination of Oxygen Atoms on Silica From 20 °C to 600 °C," Transactions of the Faraday Society, 55, 1959, 1355-61.

[12]Boenig, Herman V., Plasma Science and Technology, London: Cornell University Press Ltd., 1982.

[13]Bell, Alexis T., "Fundamentals of Plasma Chemistry," in Techniques And Applications of Plasma Chemistry, edited by Hollahan, John R. and Alexis T. Bell, New York: John Wiley & Sons, 1974.

[14]See Reference 9.